

FUSION OF GPS, INS AND ODOMETRIC DATA FOR AUTOMOTIVE NAVIGATION

M. Spangenberg*, V. Calmettes* and J.-Y. Tournet†

* SUPAERO/TéSA, 14-16 Port Saint Etienne, 31000 Toulouse, France

† IRT/ENSEEIH/TéSA - 2 rue Charles Camichel, BP 7122, 31071 Toulouse cedex 7, France

email: mariana.spangenberg@tesa.prd.fr, vincent.calmettes@supaero.fr, jean-yves.tournet@enseeiht.fr

ABSTRACT

Nowadays, accurate and reliable positioning systems are required in several applications such as safety of life or liability critical. The global positioning system (GPS) is the most common navigation system for almost any application involving localization, navigation or tracking. In particular, GPS is used intensively for automotive navigation. However, the quality of the localization task for ground vehicles is subjected to degrade in outdoor conditions. For instance, severe degradations have been observed in urban areas, when the vehicle is subjected to multipath or masking effects interfering with the satellite lines of sight. In this case, combining GPS pseudo ranges with other measurement sources is an interesting way of improving localization performance. This paper studies different fusion approaches based on differential odometry provided by wheel speed sensors (WSS) and inertial sensors such as accelerometers and gyros. Different tracking strategies based on extended and unscented Kalman filters are investigated and compared for these fusion approaches.

1. INTRODUCTION

Vehicle positioning has become a major focus of automobile industry. In urban canyon areas, different problems such as corrupted received signals or restricted/absence satellite visibility can arise. Using auxiliary sensors to mitigate this unreliable or absent information (during GPS satellite outages) is an interesting idea. These additional sensors may use dead reckoning techniques. These techniques compute the actual position of the vehicle from its known initial location by integrating differential measurements. The sensors which have been already used for vehicular navigation include gyroscopes, odometers [1], inclinometers and tilt meters among others. Another way of improving localization performance consists of using map matching techniques lately introduced as part of multi-aided navigation approaches for automobiles [2].

This paper studies the potential interest of using wheel speed sensors (WSS) in hybrid GPS. WSS are fundamental components in the antilock braking system (ABS), which will be a standard equipment in most new generation vehicles. WSS provide measurements through the vehicle controller area network (CAN). All modern cars are equipped with WSS which measure wheel angular rates and estimate the traveled distance. Therefore, coupling GPS and WSS provides a self contained positioning system that explores the already available on board information at no additional cost. A particular attention is devoted to differential odometry in this paper. In differential odometry, vehicle velocity and yaw rate are obtained by the wheel encoders on the rear undriven wheels. These informations are then used to improve localization performance. However, odometric measurements are corrupted by several errors such as wheel radius errors. Navigation performance can be improved by including these errors in the state model for their estimation [2].

Another possibility for improving navigation performance is to combine GPS and inertial navigation systems (INS) [3]. This paper focuses on a coupling approach based on a tight integration. GPS/INS hybrid systems have been used intensively in aeronautics. However, their application to the automotive industry is increasing thanks to the new low cost inertial measurement units (IMU). INS are self contained non jammable systems consisting of a 3D

accelerometer and gyros. INS errors have an exponential growth over time. Thus, GPS measurements are classically used to bound these errors during satellite visibility. On the other hand, INS offer a small correction to GPS measurements which is mostly used during GPS satellite outages. This paper studies a multi-aided navigation system integrating GPS, INS and WSS. The idea is that increasing the sensor redundancy should provide higher reliability and accuracy for the positioning system. Any failure in one sensor can be compensated by other on board sensors providing reliable measurements. For instance, during GPS satellite outages, non-holonomic constraints are applied to the vehicle trajectory. These *virtual measurements* do not differ much from the real vehicle trajectory. At the same time, they provide extra sources of measurements to make INS errors observables, improving the positioning accuracy [4]. These same holonomic constraints are applied to the vehicle attitude angles calculated from the differential odometry.

The different coupling strategies will be processed by filtering techniques based on the extended Kalman filter (EFK) and the unscented Kalman filter (UKF). The EKF is the commercially used world accepted filter for navigation. It is known to provide reasonable accuracy with a low computational cost. The EKF propagates the mean and covariance of the state assuming the state and measurement equations can be linearized. Conversely, the unscented Kalman filter (UKF) allows one to track the state mean and covariance matrix without any linearization operation [5]. The UKF approximates the state mean and covariance matrix through a set of weighted points called sigma points and propagates them through the *real* non linear measurement model. It can be shown that third order accuracy is achieved by the UKF, which considers higher order terms in the Taylor expansion than the EKF approximation [6]. Consequently, the UKF has provided significant improvement in positioning accuracy (when compared to the EKF) in several navigation applications [5], [6]. It is interesting to mention here that particle filters (PFs) are also nice alternatives to the EKF and UKF which could be used for automotive navigation. PFs capture all information regarding the state, by estimating sequentially the posterior state distribution [2]. The standard Bayesian estimators such as the minimum mean square error (MMSE) and the maximum *a posteriori* (MAP) estimators can then be derived from this state distribution. However, this paper concentrates on EKF and UKF because they provide lower computational cost filtering solutions. The comparison between the EKF and UKF will be performed by comparing the mean square errors (MSEs) of the estimates to the corresponding posterior Cramer Rao Bounds (PCRBs).

The paper is organized as follows: Section 2 presents the bases of a GPS/WSS coupling approach. The principles of INS and its coupling with GPS and WSS are explained in Section 3. Filtering strategies allowing us to estimate the vehicle position by combining different sources of measurements are presented in Section 4. Some elements regarding the computation of the PCRB for a state vector are also presented. Simulation results are shown in Section 5. Conclusions are reported in Section 6.

2. GPS/WSS HYBRIDIZATION

2.1 GPS

The GPS measurements are called pseudo-ranges (instead of ranges) since the estimated times of transmission are corrupted by different biases. The positioning equations for n_s satellites in sight at time instant t can be defined as:

$$r_i(t) = \sqrt{[X_i(t) - x(t)]^2 + [Y_i(t) - y(t)]^2 + Z_i^2(t) + b(t) + w_i(t)}, \quad (1)$$

for $i = 1, \dots, n_s$, where $r_i(t)$ is the pseudo-range between the user and the i th satellite, $[X_i(t), Y_i(t), Z_i(t)]^T$ is the position of the i th satellite in the local frame, $b(t)$ is a bias term resulting from the clock offset, $w_i(t)$ is the measurement error and $[x(t), y(t)]$ is the vehicle position to be estimated (note that the vehicle altitude is $z(t) = 0$ in this paper). These equations will be used as measurement equations in the proposed navigation solutions.

2.2 WSS

This section describes the main elements of differential odometry. The idea is to integrate informations regarding distance and yaw rate using the measurements given by the vehicle odometers. The WSS measurements will be calibrated to provide reliable information during GPS satellite outages. Figure 1 shows WSS located on the front or rear wheels. The first index of the different variables refers to the front f or rear r axes whereas the second index corresponds to the left l and right r sides of the car. Consequently, the wheel radii (resp. angular velocities) are denoted as R_{rl}, R_{rr}, R_{fl} and R_{fr} (resp. $\omega_{rl}, \omega_{rr}, \omega_{fl}$ and ω_{fr}). The other notations used in Fig. 1 are L for the length between wheels and ψ for the vehicle yaw rate (change of angle of direction). This paper focuses on velocity and yaw rate calculations using rear wheels. This choice is motivated by the fact that acceleration and deceleration have less effect on the output of these sensors.

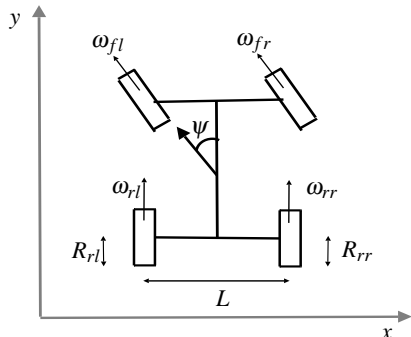


Figure 1: Illustration of WSS definition.

Assume first that the wheel radii are constant and known. The mean speed of the vehicle at time t can be computed as [2]:

$$V[\omega_{rr}(t), \omega_{rl}(t), R_{rr}, R_{rl}] = \frac{\omega_{rr}(t)R_{rr} + \omega_{rl}(t)R_{rl}}{2}. \quad (2)$$

The yaw rate of the vehicle can be calculated similarly as a function of the angular velocities of each wheel (3). By neglecting side slip effects (see [7] for more details) and modeling the vehicle as a rigid body, the vehicle yaw rate at time t expresses as

$$\dot{\psi}(t) = h[\omega_{rr}(t), \omega_{rl}(t), R_{rr}, R_{rl}] = \frac{\omega_{rr}(t)R_{rr} - \omega_{rl}(t)R_{rl}}{L}. \quad (3)$$

Errors in the wheel radii will have a strong impact on localization accuracy when getting propagated through the angle and velocity expression. Indeed, any non corrected error will result in an accumulative increasing error. A usual way of mitigating the effects of radius variations $\delta R_{rr}(t)$ and $\delta R_{rl}(t)$ is to include them in the state vector, as shown in the next section.

2.3 GPS/WSS Integration

If the wheel radii were constant, the vehicle speed and yaw rate would be related to $\omega_{rr}(t)$ and $\omega_{rl}(t)$ by the following equations:

$$\dot{x}(t) = -V[\omega_{rr}(t), \omega_{rl}(t), R_{rr}, R_{rl}] \sin[\psi(t)] + v_x(t), \quad (4)$$

$$\dot{y}(t) = V[\omega_{rr}(t), \omega_{rl}(t), R_{rr}, R_{rl}] \cos[\psi(t)] + v_y(t), \quad (5)$$

$$\dot{\psi}(t) = h[\omega_{rr}(t), \omega_{rl}(t), R_{rr}, R_{rl}] + v_\psi(t), \quad (6)$$

where $v_x(t), v_y(t)$ and $v_\psi(t)$ are white noise sequences. When the wheel radii are time varying, the components R_{rr} and R_{rl} have to be replaced in (4), (5) and (6) by their time-varying counterparts $R_{rr} + \delta R_{rr}(t)$ and $R_{rl} + \delta R_{rl}(t)$. This yields the following continuous-time state model

$$\dot{x}(t) = -V[\omega_{rr}(t), \omega_{rl}(t), \delta R_{rr}(t), \delta R_{rl}(t)] \sin[\psi(t)] + v_x(t),$$

$$\dot{y}(t) = V[\omega_{rr}(t), \omega_{rl}(t), \delta R_{rr}(t), \delta R_{rl}(t)] \cos[\psi(t)] + v_y(t),$$

$$\dot{\psi}(t) = h[\omega_{rr}(t), \omega_{rl}(t), \delta R_{rr}(t), \delta R_{rl}(t)] + v_\psi(t),$$

$$\delta \dot{R}_{rr}(t) = v_r(t), \quad \delta \dot{R}_{rl}(t) = v_l(t),$$

where $v_r(t)$ and $v_l(t)$ are white noise sequences. Note that this model considers the wheel radius errors as random constants whose derivatives are Gaussian white noises. The previous state equations are completed by a GPS clock offset dynamic model defined as:

$$\dot{b}(t) = d(t) + v_b(t), \quad \dot{d}(t) = v_d(t), \quad (7)$$

where $b(t)$ denotes the GPS receiver clock offset in meters, $d(t)$ is the derivative of $b(t)$ and $v_b(t), v_d(t)$ are white noise sequences.

The resulting continuous time state vector for GPS/WSS integration is composed of the vehicle position, angle of direction, radii and clock parameters at time t :

$$\chi_t = [x(t), y(t), \psi(t), \delta R_{rr}(t), \delta R_{rl}(t), b(t), d(t)]^T \in \mathbb{R}^7. \quad (8)$$

This paper assumes that the wheel speeds, radius offsets and noises are piecewise constant. As a consequence, the previous continuous-time state model can be classically discretized by replacing derivatives by finite differences, e.g. $\dot{x}(t)$ by $\frac{x((n+1)T_s) - x(nT_s)}{T_s}$, where T_s is the sampling period.

3. GPS/INS/WSS HYBRIDIZATION

3.1 INS

INS are self-relying and autonomous systems which have been widely used in navigation applications. They are composed of an IMU with inertial sensors (accelerometers and gyrometers). The IMU is coupled with a computer that provides the mobile with its position, velocity and attitude angles. The accelerometers deliver a non gravitational acceleration (also referred to as specific force f^p) and the gyrometers measure the rotation rate of the sensor cluster Ω_{ip}^p in order to keep track of the vehicle orientation. As explained before, this paper assumes that the vehicle altitude is $z(t) = 0$, or equivalently that the vehicle is equipped with 2D accelerometers and gyrometers. Moreover, we use the following notations:

R_{a2b} : rotation matrix from frame a to frame b,

p^b : location of the vehicle in the frame b,

Ω_{ab}^b : rotation rate from frame a to frame b, resolved in frame b,

v_a^b : velocity relative to frame a, resolved in frame b.

The subscripts and superscripts refer to the different coordinate frames, i.e., i : inertial frame, e : earth centered earth fixed frame, n : local geographic frame, p : platform frame. The differential equations relating the measured quantities to the dynamics are defined as follows:

$$\dot{v}_e^n = R_{p2n} f^p + g^n - (\Omega_{en}^n + 2\Omega_{ie}^n) v_e^n - [\Omega_{ie}^n]^2 p^n, \quad (9)$$

$$\dot{p}^n = \begin{pmatrix} \dot{\lambda} \\ \dot{\phi} \end{pmatrix} = \begin{pmatrix} \frac{1}{R_\lambda} & 0 \\ 0 & \frac{1}{R_\phi \cos \lambda} \end{pmatrix} v_e^n, \quad (10)$$

where g^n is the gravitational acceleration in the local geographic frame, λ and ϕ are the latitude and longitude of the mobile, $v_e^n(t) = [\dot{y}(t), \dot{x}(t)]$ is defined in the same frame of the WSS showing the north and east velocity, R_λ is the earth radius of curvature in a meridian at a given latitude and R_ϕ is the transverse radius (we consider the WGS84 model for which the earth is an ellipsoid). These equations are integrated to obtain the vehicle position and velocity. This integration will entail a drift in stand-alone INS estimates due to a bias affecting the INS measurements (denoted as b_a for the accelerometer bias and as b_g for the gyroscope bias). These errors affecting the position accuracy can be reduced by coupling the INS with the GPS and WSS outputs. In the following sections, the commonly used GPS/INS coupling approach will be first introduced. An extension to the hybrid system GPS/WSS/INS will then be discussed.

3.2 Multi-sensor integration

3.2.1 GPS/INS

The common GPS/INS coupling techniques use the GPS pseudorange measurements to correct the INS errors in order to obtain reliable position estimation. This procedure is interesting since the integrated system can still rely on INS outputs in absence of GPS measures (due for instance to masking). The errors of the INS system are defined as the difference between the actual INS parameter values and their estimations $\delta X = X - \hat{X}_{INS}$. The state model describing the INS error dynamic behavior can be obtained by linearizing the *ideal equations* around the INS estimates [9]. The state vector is usually augmented with systematic sensor errors:

$$\chi = (\delta v_e^n, \delta \rho, b_a, b_g, \delta p^n, b, d)^T \in \mathbb{R}^9, \quad (11)$$

where δp^n and δv_e^n contain the position and velocity errors, $\delta \rho$ is the inertial yaw rate error, b_a and b_g are the accelerometer and gyroscope biases, b denotes the GPS receiver clock offset in meters and d its derivative. The dynamic model used in this paper for (b, d) has been defined in (7). The INS state equations can be defined as follows (see [3] or [9] for more details):

$$\delta \dot{p} = -\delta \Omega_{in}^n - S(\Omega_{in}^n) \delta \rho + R_{p2n} \delta \Omega_{ip}^n \quad (12)$$

$$\delta \dot{v}_e^n = R_{p2n} b_a + S(\delta \rho) f^n - S(\Omega_{en}^n + 2\Omega_{ie}^n) \delta v_e^n + \delta g^n - S(\delta \Omega_{en}^n + 2\delta \Omega_{ie}^n) v_e^n, \quad (13)$$

$$\delta \dot{p}^n = S(\Omega_{en}^n) \delta p^n + \delta v_e^n, \quad (14)$$

where $S(u)$ is the skew-symmetric matrix such that $S(u)y = u \wedge y$ and $u \wedge y$ denotes the cross product between vectors u and y [3, p. 292]. Note that the vectors appearing in the INS state equations above are obtained by adding a third component equal to 0 corresponding to the altitude. The measurement equation for the GPS/INS system is still given by the pseudorange (1) where $(x(t), y(t))$ are obtained from the geodetic corrected measurements $(\lambda + \delta \lambda, \phi + \delta \phi)_{INS}$ in the rectangular coordinate system.

3.2.2 GPS/INS/WSS

Integrating GPS, INS and WSS is a challenging and interesting navigation problem. This section first considers GPS/INS integration as explained above and introduces WSS to enhance the accuracy on the given position estimations. As already explained, the outputs from the rear WSS provide the absolute velocity V in the vehicle heading direction, and its yaw rate $\dot{\psi}$. These will be used as measurements to update the filter. For this, the state vector (11) is augmented by radius errors affecting the WSS yielding

$$\chi = (\delta v_e^n, \delta \rho, b_a, b_g, \delta p^n, b, d, \delta R_{rr}, \delta R_{rl})^T \in \mathbb{R}^{11}. \quad (15)$$

The idea is to use WSS measurements to further correct the INS errors. Note that a frame transformation is necessary to compare INS and WSS data. In the presence of GPS, the WSS contribution is very small. However, this contribution is crucial during GPS satellite outages since it allows one to correct the INS growing errors.

The proposed GPS/INS/WSS integration considers non-holonomic constraints for the WSS measurement vector as in [4]. The idea is to have the maximum number of *measurements* available during GPS outages. Assume that the side slip effects can be neglected as in [7], the altitude can be set to 0 in (1) and there is no misalignment between the body frame and the vehicle. Consequently, the *virtual* measurements provided by the non-holonomic constraints will help to keep track of INS errors. The WSS measurement equation for the yaw rate is given by,

$$\psi_{WSS} - \rho_{INS} = h_\psi(\delta R_{rr}, \delta R_{rl}, \delta \rho), \quad (16)$$

where $h(\cdot)$ is the difference between the radius errors propagated through the yaw rate expression (3) and the INS attitude errors:

$$h_\psi(\delta R_{rr}, \delta R_{rl}, \delta \rho) = \frac{\omega_{rr} \delta R_{rr} - \omega_{rl} \delta R_{rl}}{L} + \delta \rho. \quad (17)$$

A frame transformation has to be used to compare the velocities given by each system appearing in (2) and (9). This paper converts the INS velocities to the vehicle frame (an alternative would be to express WSS velocities in the navigation frame). In this case, the velocity WSS measurement equation can be written

$$(V, 0)_{WSS}^T - R_{p2n}^T (v_e^n)_{INS} = h_V(\delta R_{rr}, \delta R_{rl}, \delta \rho, \delta v_e^n), \quad (18)$$

where

$$h_V(\cdot) = \frac{\omega_{rr} \delta R_{rr} + \omega_{rl} \delta R_{rl}}{2} + R_{p2n}^T \delta v_e^n + R_{p2n}^T S(v_e^n) \delta \rho. \quad (19)$$

4. FILTERING TECHNIQUES

This section recalls standard filtering techniques which provide estimates of the state vector χ_t from the following state-space model:

$$\chi_t = A_t \chi_{t-1} + v_t, \quad r_t = h(\chi_t) + u_t,$$

where χ_t is the state vector, A_t is the state model propagation matrix, r_t is the measurement vector (pseudo-ranges) and h_t is the non linear function relating the pseudo-ranges to the state vector. The noise sequences v_t and u_t are supposed to be independent white Gaussian with covariances matrices Q_t and R_t .

4.1 EKF

The EKF proceeds by linearizing the model about the latest estimate to meet the Kalman Filter assumptions. The state space model defined above is then classically approximated as follows:

$$\begin{cases} \chi_t & = A_t \chi_{t-1} + v_t \\ r_t & \simeq H_t (\chi_t - \hat{\chi}_{t|t-1}) + h_t(\hat{\chi}_{t|t-1}) + u_t, \end{cases} \quad (20)$$

where $H_t = \frac{dh_t(x)}{dx} \Big|_{x=\hat{\chi}_{t|t-1}}$. Consequently, the conditional probability of the state $p(\chi_t | r_{1:t})$ can be estimated by a Gaussian probability density function whose mean $\hat{\chi}_{t|t}$ and covariance $P_{t|t}$ can merely be computed by Kalman recursions.

4.2 UKF

The UKF does not need to linearize the non linear measurement equation to determine the covariance matrix of the random state vector. For this purpose, a set of sigma points with appropriate weights is deterministically chosen so as to capture the mean and covariance of this random vector up to a third order accuracy. More precisely, consider a random vector x with mean \bar{x} and covariance

matrix P_x . The sigma points and the weights associated to \mathbf{x} are defined as follows:

$$X_0 = \bar{x}, \quad W_0 = \frac{\lambda}{(n + \lambda)} \quad (21)$$

$$X_i = \bar{x} + \sqrt{(n + \lambda)P_x}, \quad W_i = \frac{1}{2(n + \lambda)} \quad (22)$$

$$X_{i+n} = \bar{x} - \sqrt{(n + \lambda)P_x}, \quad W_{i+n} = \frac{1}{2(n + \lambda)} \quad (23)$$

where $i = 1, \dots, n$ and n is the dimension of the state vector. The parameter λ is a scaling parameter. The mean and covariance matrix of the Gaussian vector $\mathbf{y} = h(\mathbf{x})$ can then be approximated as follows:

$$\bar{y} = \sum_{i=0}^{2n} W_i Y_i, \quad P_y = \sum_{i=0}^{2n} W_i (Y_i - \bar{y})(Y_i - \bar{y})^T,$$

where $Y_i = h(X_i)$ is the result of each sigma point X_i undergoing the non linear transformation h .

In the general formulation, the state vector is *augmented* by concatenating the original state vector with the state and measurement noises [5]. However, this concatenation is not required here, since the state and measurement noises are additive [10]. In this way, the size of the sigma points is reduced, enabling a more efficient algorithm. For the rest of the filtering process, the UKF algorithm follows the principles of the Kalman Filter adapted to the unscented transform. The reader is invited to consult [10] for a detailed description of the UKF, specially in the additive zero mean noise case.

4.3 Posterior Cramer-Rao Bound (PCRB)

The PCRB provides a lower bound on the MSEs of the state estimates. It can be viewed as a reference to which the state MSEs of suboptimal algorithms can be compared. The PCRB is often referred to as the Bayesian version of the Cramer-Rao bound. The recursive formulas allowing to compute the PCRB are detailed in [11]. All expectations appearing in these formulas have been estimated by averaging the results over several Monte Carlo runs. This paper focuses on the PCRB for the horizontal INS position error denoted by HPCRB, since the vehicle altitude is supposed to be 0. We recall here that the horizontal position error can be defined as functions of the latitude $\delta\lambda$ and longitude $\delta\phi$ inertial errors by $HE = (R\delta\lambda)^2 + (R\delta\phi \cos\lambda)^2$, where R stands for the earth radius.

5. SIMULATION RESULTS

Several simulations have been conducted to compare the different coupling techniques. All results presented in this section have been averaged over 25 Monte-Carlo runs (note that the vehicle trajectories differ from one Monte Carlo run to another). An example of the simulated vehicle dynamics corresponding to an acceleration variance of $5m/s^2$ is depicted in Fig. 2. The pseudo-range measurement accuracy for the GPS signal is 12m (i.e. the standard deviation of $w_i(t)$ is equal to 12m). The WSS parameters have been adjusted according to standard vehicles, i.e. $L = 1.8m$ and $R_{rr} = R_{rl} = 0.23m$. INS errors have been simulated according to an HG1700 tactical IMU for realistic purposes [4]. The standard deviations of the noise components $v_V(t), v_x(t), v_y(t), v_\psi(t)$ and $v_r(t), v_l(t)$ are summarized in the following table

	V	x	y	ψ	δR
σ	0.04 m/s	0.04 m	0.04 m	0.06 m	10^{-7} m

A scenario with full GPS visibility is first presented. The GPS receiver is assumed to view 7 satellites in line of sight (LOS). Figure 2 shows an example of real trajectory followed by the vehicle and the estimated position obtained when using WSS only (WSS trajectory). The estimated trajectory resulting from the coupling approach

GPS/WSS (Filtered trajectory) is also depicted. The coupling between GPS and WSS is clearly necessary for this example. Fig. 3 shows the positioning errors for the GPS/WSS coupling approach which are compared to the corresponding PCRB. These errors fluctuate from 10 to 15 meters. Note that the coupling technique performs similarly when using the EKF or the UKF. The vehicle dynamics is sufficiently slow for this example to linearize efficiently the measurement equation (1). Therefore the UKF doesn't show any improvement over the EKF. Note also that the hybridization approach reaches almost the best achievable precision, provided by the Posterior Cramer Rao bound. Similar results obtained for the GPS/INS/WSS hybridization can be observed in Figs. 4 and 5. A comparison between both coupling techniques shows that the GPS/INS/WSS outperforms the GPS/INS approach. Adding INS measurements to GPS and WSS data results in improved accuracy. For instance, the GPS/INS/WSS positioning errors fluctuate from 5 to 10 meters.

For further comparisons, a more realistic urban scenario is presented with partial GPS availability. The idea is to observe the behavior of the different coupling techniques with a reduced number of visible GPS satellites. For this, we have simulated a 30s time interval during which only two GPS satellites are visible, followed by a 30s GPS outage (both indicated by vertical black lines in Fig. 6). Fig. 6 compares the positioning errors obtained for the different coupling and filtering strategies for this example. The GPS/INS/WSS coupling clearly outperforms GPS/WSS during limited GPS visibility and GPS outages. The use of INS helps to keep a bound over the positioning errors, avoiding losing track of the vehicle. Consequently, GPS/INS/WSS hybridization provides reliable positions during longer periods than the GPS/WSS system. Note also that a slight improvement is observed with the UKF (versus the EKF) when regaining full GPS visibility.

Another way of comparing the different coupling strategies is to analyze the corresponding horizontal position PCRBs for different numbers of LOS satellites. Table 1 shows that the asymptotic horizontal error PCRBs corresponding to the GPS/WSS coupling tend to diverge over time when working with a small number of satellites, contrarily to the GPS/INS/WSS hybridization. Note that there is a significant gain when passing from 5 to 6 satellites in the GPS/WSS case. Indeed, the sixth satellite has a very good visibility (in terms of Dilution of Precision) for this GPS constellation.

6. CONCLUSIONS

This paper presented two different coupling techniques referred to as GPS/WSS and GPS/INS/WSS. The GPS/WSS approach used the already existing wheel speed sensors from the automobile ABS. Both the yaw rate and velocity of the vehicle were obtained by differential odometry. In this way an economic self contained solution was provided for vehicle navigation. On the other hand, the widely used aeronautics GPS/INS approach was adapted to land vehicle navigation, by including WSS measurements.

Simulation results showed a good performance for both systems. However, the GPS/INS/WSS outperformed the GPS/WSS accuracy by approximately 5 meters. To highlight the sensor contributions to tracking purposes, hostile conditions (limited GPS visibility and GPS outages) were simulated. Combining GPS with different sensors enabled the system to provide a reliable position estimation during these hostile conditions. The asymptotic PCRBs for both hybrid approaches under varying numbers of LOS GPS satellites were also computed. The stability in terms of accuracy for the GPS/INS/WSS system appeared superior to GPS/WSS. Having more dead reckoning measurement sources make the GPS/INS/WSS system more able to work efficiently in urban areas affected by limited GPS availability. The measurement equation associated to the proposed navigation state space model is nonlinear. Two filtering techniques based on the EKF and UKF were compared for this navigation problem and provided similar results. Land vehicles are subjected to slow varying dynamics yielding similar performance for both techniques.

Further investigations include the development of fusion strategies based on low cost sensors. Different approaches can be explored and evaluated. The first one consists of examining the interest of a pressure sensor used as an altimeter to provide vertical accuracy improvement. The second technique takes the best advantage of the tire monitoring system which is going to become standard for all vehicles. Finally an image-aided navigation system might be investigated.

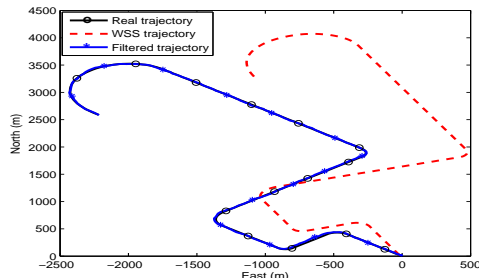


Figure 2: Example of an actual and estimated trajectory (GPS/WSS).

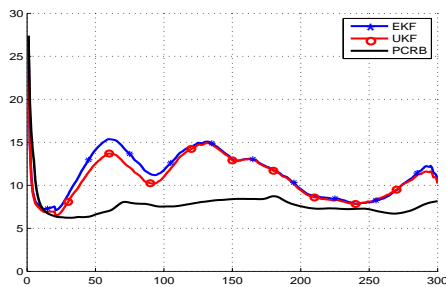


Figure 3: Horizontal position errors (GPS/WSS).

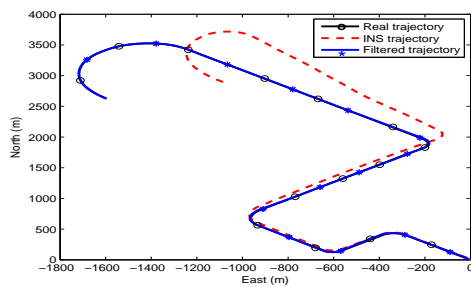


Figure 4: Actual and estimated trajectories (GPS/INS/WSS).

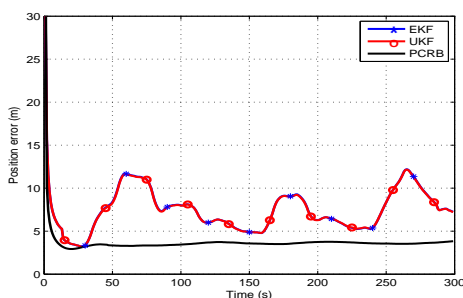


Figure 5: Horizontal position errors (GPS/INS/WSS).

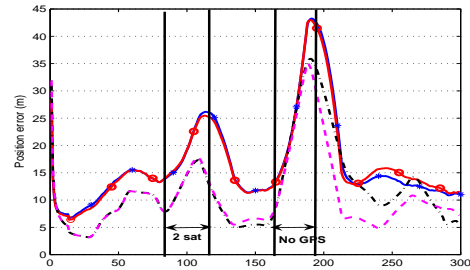


Figure 6: Position errors for urban scenario. (a) GPS/WSS approach with EKF and UKF (solid lines with \circ and $*$). (b) GPS/INS/WSS approach with EKF (dash-dotted) and UKF (dotted lines).

N of LOS sat.	GPS/WSS	GPS/INS/WSS
1	div	60 m
2	div	17 m
3	21 m	8 m
4	18.6 m	5 m
5	16 m	4.7 m
6	10 m	4 m
7	9.5 m	3.7 m

Table 1: Asymptotic Horizontal PCRBs.

REFERENCES

- [1] J. Stephen, "Development of a multi-sensor GNSS based vehicle navigation system," Master's thesis, University of Calgary, Calgary, Canada, 2000.
- [2] N. Svenzén, "Real time implementation of MAP aided positioning using a Bayesian approach," Master's thesis, University of Linköping, Linköping, Sweden, 2002.
- [3] J. A. Farrell and M. Barth, *The Global Positioning System and Inertial Navigation*. New York: McGraw-Hill, 1999.
- [4] J. Gao, M. G. Petovello, and M. E. Cannon, "Development of precise GPS/INS/Wheel Speed Sensor/yaw rate sensor integrated vehicular positioning system," in *Proc. of ION NTM-06*, (Monterey, CA), Jan 2006.
- [5] S. Julier and J. Uhlmann, "Unscented Filtering and Nonlinear Estimation," *Proc. of the IEEE*, vol. 92, pp. 401-422, 2004.
- [6] R. van der Merwe, *Sigma-Point Kalman Filters for Probabilistic Inference in Dynamic State-Space Model*. PhD thesis, University of Stellenbosch, Oregon, USA, 2004.
- [7] M. Enquist, "Aspects of high precision estimation of vehicle dynamics," Master's thesis, University of Linköping, Linköping, Sweden, Dec. 2000.
- [8] A. Giremus, A. Doucet, V. Calmettes, and J.-Y. Tournet, "A Rao-Blackwellized Particle Filter for INS/GPS integration," in *Proc. ICASSP-04*, (Montreal, Canada), May 2004.
- [9] E. Wan and R. van der Merwe, "The Unscented Kalman Filter," in *Kalman Filtering and Neural Networks* (S. Haykin, ed.), pp. 221-280, Wiley, 2001.
- [10] N. Bergman, "Posterior Cramer-Rao Bounds for Sequential Estimation," in *Sequential Monte Carlo methods in practice* (A. Doucet, N. de Freitas, and N. Gordon, eds.), pp. 321-338, New York: Springer Verlag, 2001.